EXTENSION OF THE PERFORMANCE OF LAPLACE DECONVOLUTION IN THE ANALYSIS OF FLUORESCENCE DECAY CURVES

MARCEL AMELOOT AND HUBERT HENDRICKX
Division of Biophysics, Limburgs Universitair Centrum, Universitaire Campus, B-3610 Diepenbeek, Belgium

ABSTRACT The original Laplace deconvolution of luminescence data, obtained with pulsed systems, is reviewed. The system of equations from which the luminescence parameters can be determined is generalized for the case that describes the relaxation by a sum of exponentials. Artifacts such as scatter and time-shift can be taken into account. A modification of the original method that eliminates the iterative procedure in the estimation of the cut-off correction is suggested. This modified Laplace method is no longer restricted to the cases where the cut-off error is rather small and the exciting flash has a low tail. The possibility of the combination of several discrete experiments in a single Laplace deconvolution, without introducing new parameters or normalization factors, is shown. The merits of this combination method are demonstrated on a time-resolved depolarization experiment.

INTRODUCTION

Luminescence decay data obtained with pulsed systems do not represent the true decay because of the finite width of the excitation profile and the finite instrumental response time. If the various instrumental response functions are the same for both excitation and emission, then the observed decay profile, $g(t)$, is the convolution product of the measured excitation profile, $l(t)$, with the δ-pulse response of the luminescent system $f(t, \theta)$, i.e.,

$$g(t) = \int_0^t l(u) f(t - u, \theta) du \equiv l(t) * f(t, \theta). \quad (1)$$

In the actual measurement, the relation expressed by Eq. 1 is evaluated at a set of some fixed values of t, the independent variable, which is assumed not to have any errors. The problem of deconvolution has been investigated and reviewed (1, 2).

One of the most popular methods is the iterative reconvolution technique by means of a nonlinear least-squares (NLLS) algorithm. In this method a model $f(t, \theta)$ has to be proposed a priori, and the parameters $\{\theta_j\}$ are determined by minimizing

$$\chi^2 = \sum_{i=1}^{N} \frac{1}{\sigma_i^2} [y^o(t_i) - y^c(t_i, \theta)]^2$$

in which $y^o(t_i)$ are the observed values and $y^c(t_i)$ are the calculated values of the convolution product in an interval of width, W, centered at the values t_i of t; σ_i represents the error of the i^{th} data point. When the luminescence decay is measured by the single photon counting (SPC) method and the channel contents are high enough, the Gaussian approximation is valid so that $\sigma_i^2 \approx y^o(t_i)$. In most cases, the response $f(t, \theta)$ can be described adequately by a sum of exponentials,

$$f(t, \theta) = \sum_{j=1}^{n} a_j e^{-t/\tau_j}, \quad (2)$$

where $\theta = \{a_1, \ldots, a_n, \tau_1, \ldots, \tau_n\}$. Because of the nonlinearity of $f(t, \theta)$ in $\{\tau_j\}$, the procedure of the minimalization of χ^2 requires an adequate set of starting values $\{a_p, \tau_p\}$. The implications of this nonlinearity on a statistical analysis have been described elsewhere (3).

A deconvolution technique, which does not need a set of starting values, can be provided by the Laplace transformation method. Because the SPC technique can obtain a high signal-to-noise ratio, the use of this analytic method is justified.

The Laplace deconvolution has been described originally by Helman (4) and has been extended by Gafni et al. (5). The latter also accounted for distortions of the data such as a scatter component in the decay curve and a time-shift of the decay relative to the exciting flash.

One of the most severe difficulties of the Laplace deconvolution is that the transformation requires an integration over time to infinity, whereas the time window of the measured decay is restricted. Because of this cut-off, Gafni et al. (5) suggested an iterative procedure for calculating the Laplace transform of $g(t)$. The present paper describes how this cut-off problem can be circumvented by an elimination procedure. The merits of this method are demonstrated on simulated and real data sets. It is shown that, where the original Laplace method fails, the modified method can have performances that are

comparable with the iterative reconvolution method. Moreover, it will be shown that the modified Laplace deconvolution technique provides a unique method of combining time-resolved decay measurements in the time domain without introducing new parameters as required by the NLLS method. The general conclusion will be that this new Laplace method without iteration provides a robust method for extracting parameters from experimental decay curves. In the subsequent sections, the original method of Gafni et al. (5) is briefly reviewed and a more general algorithm presented. The alternative method is then proposed and compared with the former and the NLLS method.

THEORY

Laplace Deconvolution Method

Because $g(t)$ and $l(t)$ should be equal to zero for $t < 0$, the Laplace transform will be considered on $[0, \infty[$. The transformation with parameter s of Eq. 1 yields $G(s) = L(s)\,F(s)$, where $G(s)$, $L(s)$, and $F(s)$ denote the Laplace transforms of $g(t)$, $l(t)$, and $f(t, \theta)$, respectively. It will be supposed further on that $f(t, \theta)$ is described by Eq. 2. Because of the linearity of the Laplace operator $F(s)$ can be written as

$$F(s) = \sum_{i=1}^{n} \frac{a_i}{s + \frac{1}{\tau_i}},$$

providing the equality

$$\frac{G(s)}{L(s)} = \sum_{i=1}^{n} \frac{a_i}{s + \frac{1}{\tau_i}}. \tag{3}$$

By calculating $2n$ Laplace transforms (s, real and positive) of $g(t)$ and $l(t)$, we determine $2n$ nonlinear equations like Eq. 3 from which a_i and τ_i are solved.

However, the experimental curves are only defined for a finite time window $(0,T)$ and, in general, do not vanish in the last data channel at time T. This means that Eq. 3 must be corrected for this cut-off error. One may write

$$G(s) = \int_0^T g(t)\, e^{-st}\, dt + \int_T^\infty g(t)\, e^{-st}\, dt$$
$$= g^T(s) + G^\infty(s).$$

The cut-off correction $G^\infty(s)$ is completely determined by the assumed extension of the excitation profile $l(t)$ on $[T, \infty[$. Although several extensions are valid, an obvious choice is to set $l(t)$ equal to zero for $t > T$. This means that $L(s) = L^T(s)$. In that case, $G^\infty(s)$ can be described as

$$G^\infty(s) = e^{-sT} \sum_{i=1}^{n} \frac{c_i^T}{s + \frac{1}{\tau_i}} \tag{4}$$

in which c_i^T is the contribution of the i^{th} component to the last channel of the measured decay, i.e.,

$$c_i^T = \int_0^T l(u)\, a_i\, e^{-(T-u)/\tau_i}\, du.$$

An alternative expression for $G^\infty(s)$ may be obtained by noting that

$$c_i^T = a_i\, e^{-T/\tau_i} \int_0^T l(u)\, e^{u/\tau_i}\, du = a_i\, L^T\left(-\frac{1}{\tau_i}\right),$$

and hence

$$G^\infty(s) = e^{-sT} \sum_{i=1}^{n} \frac{a_i\, e^{-T/\tau_i}\, L^T\left(-\frac{1}{\tau_i}\right)}{s + \frac{1}{\tau_i}}. \tag{5}$$

Gafni et al. (5) proposed an iterative procedure for calculating the corrected transforms. The solution of a set of Eq. 3 with $G^T(s)$ and $L^T(s)$ leads to a first approximation of a_i and τ_i, which in turn are used in calculating $G^\infty(s)$ according to Eq. 4 or 5. The transforms of $g(t)$ can then be corrected, which will lead to a new set of estimates for the parameters, and this procedure is repeated until some convergence criterion is satisfied.

Instrumental artifacts, such as scatter and time-shift, may be corrected with this deconvolution method by modifying Eq. 3. The amount of scattered lamplight, S_c, can be calculated by considering

$$\frac{G(s)}{L(s)} = \sum_{i=1}^{n} \frac{a_i}{s + \frac{1}{\tau_i}} + S_c. \tag{6}$$

When the decay curve is shifted to longer times due to effects in the detection photomultiplier, the time-shift Q, $Q > 0$, may be estimated by solving

$$\frac{G(s)}{L(s)} = e^{-Qs} \sum_{i=1}^{n} \frac{a_i}{s + \frac{1}{\tau_i}}. \tag{7}$$

The best way to consider the time-shift in the analysis of multiexponential decays is to determine Q from a single exponential standard at the same wavelengths. The solutions of Eqs. 3, 6, and 7, with expressions specific for $n = 1$ and 2, have been described by Gafni et al. (5). The aim of the present paper is first to propose a general solution for n components. In a second approach, an alternative for the cut-off problem is suggested.

General Solution With Iteration: Laplace Method 1 (LAP1)

The solution of Gafni et al. (5) seems not to take special precautions to assure numerical stability and requires separate expressions for $n = 1$, 2, and 3. A more general solution is presented in Appendix A. The suggested procedure, efficiently programmable on a computer, can be outlined as follows. The system of equations nonlinear in a_i and τ_i can be converted into a system of equations linear in the functions $D_i(\tau)$ and $E_i(a, \tau)$ as defined in Appendix A. Common numerical procedures can then be used for an accurate determination of D_i and E_i. Once $\{\tau_i\}$ are determined from D_i, $\{a_i\}$ can be readily obtained from E_i.

When unexpected negative parameter values result from the first step in the analysis, another choice for the transformation parameters, s_j, could be advised. However, we found that in many cases the first set of s_j can be maintained, provided that the decay component with the wrong parameter values is ignored in the calculation of the cut-off correction. Use Eq. 4 instead of Eq. 5 in the calculation of the correction to avoid overflow caused by $L^T(-1/\tau_i)$. The original Laplace deconvolution, implemented with the general solution and the restriction in the calculation of the cut-off correction, will be denoted further by LAP1.

Alternative for the Cut-Off Problem: Laplace Method 2 (LAP2)

In the case of a large cut-off error, LAP1 may not yield a valid first approximation for a_i and τ_i for multi-exponential decays, or the iteration procedure will take a long computing time. These shortcomings can be remedied by using only $G^T(s)$ and $L^T(s)$ and by considering c_i,

$$c_i = e^{-T/\tau_i} L^T\left(-\frac{1}{\tau_i}\right),$$

in Eq. 5 as a new parameter, so that an iteration is not necessary. The equations to be solved are then given by

$$\frac{G^T(s)}{L^T(s)} = \sum_{i=1}^{n} \frac{a_i}{s + \frac{1}{\tau_i}}\left(1 - \frac{e^{-sT}c_i}{L^T(s)}\right). \tag{8}$$

The scatter and the time-shift may be introduced in the same way as in LAP1. This alternative procedure is outlined in Appendix B and will be denoted further by LAP2. It will be shown that the use of LAP2 extends the applicability of the Laplace deconvolution beyond the cases where the truncation error is insignificant, and eliminates the necessity of an iteration resulting in a very fast computing algorithm.

Combination of Experiments

The alternative Laplace deconvolution, LAP2, leads also to performances that were not so easily realized before. In this new approach, several time-resolved experiments can be combined in a single deconvolution. When the pre-exponential factors are first eliminated from Eq. 8, only the functions of the lifetimes will remain. Hence normalization factors between the various data sets are not required in contrast to NLLS. The combination procedure is outlined in Appendix C.

Because LAP2 eliminates the cut-off error, decay experiments performed with different time windows may be combined to obtain a high accuracy in resolving multi-exponentials with extreme parameter values. Another typical application of this combination method is the data analysis of a time-dependent depolarization experiment. In this measurement, the time course of the fluorescence emission is analyzed into the parallel and perpendicular components, $i_\parallel(t)$ and $i_\perp(t)$, with respect to the polarization of the excitation light. The emission anisotropy is defined as

$$r(t) = \frac{i_\parallel(t) - i_\perp(t)}{i_\parallel(t) + 2\,i_\perp(t)}.$$

In general, the decay of the emission anisotropy in an isotropic environment is described by a sum of exponentials (6)

$$r(t) = \sum_{j}^{m} \beta_j\, e^{-t/\phi_j}.$$

If the rotational motion of the fluorescent molecule is restricted, a constant (r_∞) will appear in this expression (7). The two polarization components can be expressed as

$$i_\parallel(t) = \frac{f(t)}{3}\,[1 + 2\,r(t)]$$

$$i_\perp(t) = \frac{f(t)}{3}\,[1 - r(t)].$$

Both data sets are linear combinations of $n(m + 1)$ exponential terms with the same parameters.

In an experimental environment, the two data sets are mismatched because of fluctuations in lamp intensity, different duration of measurement of each component, and unequal characteristics of the SPC optics with respect to the polarization directions. It is described in Appendix D how the combination possibility of LAP2 can be used to determine the fluorescence and the anisotropy parameters without the knowledge of this matching factor. In practice, the number of exponentials, m, in the anisotropy $r(t)$ is restricted to one or two. In isotropic solvents, this may correspond to an isotropic rotator or to special cases of a rigid ellipsoid (6). However, in an anisotropic environment (e.g., lipid bilayer) the description of the anisotropy, $r(t)$, by one or two exponential relaxations and a constant can only be an approximate model (7).

MATERIALS AND METHODS

Instrumentation

The fluorescence decays were measured by means of a conventional SPC-apparatus. The optical part and the detector (Mullard 56 DUVP/03) were purchased from Applied Photophysics Ltd. (London, United Kingdom). The NIM-electronics were delivered by Canberra Industries (Meriden, CT) and Ortec (Oak Ridge, TN). The multichannel analyzer was directly connected to a PDP 11/34 (Digital Equipment Corp., Malboro, MA). For the decay measurement of the probe embedded in vesicles and the depolarization experiment, HNP'B dichroic film polarizers (Polaroid Corp., Cambridge, MA) are inserted in the excitation and the emission path. In the case where the excitation light was scattered sufficiently by the fluorescence solution itself, the fluorescence decay and the excitation profile were collected almost simultaneously under computer control via CAMAC (computer-automated measurement and control) interfacing. This ensured compensation for shape and timing drifts of the exciting flash (8).

Real Decay Data

A first set of decay measurements was performed on a degassed solution of high-pressure liquid chromatography (HPLC) purified 1,3-di(β-nafthoxy)-propane in iso-octane. The sample was excited at 280 nm and the fluorescence of the monomer was measured at 335 nm. From a previous study (9), it could be concluded that the monomer fluorescence decay of this system is described by a sum of three exponentials with well separated decay constants below 20°C. When the temperature is increased the separations between the decay constants decrease so that a decay measured at room temperature provides a real test case for a deconvolution algorithm. A satisfactory fit could only be obtained with three relaxation times with values well in line with the results of the previous study (3). A second real decay was obtained by measuring the fluorescence of bis-[9-(10-phenyl) anthrylmethoxy] methane (DPAA) embedded in unilamellar vesicles of dipalmitoylphosphatidylcholine (DPPC) at 33°C. The vesicles were prepared as described by Chen (10) except that the probe molecule was added to the lipids in chloroform prior to the evaporation step. The probe to lipid ratio was 1:500. The excitation and emission wavelength were 358 nm and 425 nm, respectively. To measure the total fluorescence, the excitation light was vertically polarized and the emission was monitored through an analyzer oriented at 55° with respect to the vertical. Finally, the combination of data sets will be demonstrated with a time-dependent depolarization experiment performed on rhodamine 6G in propylene glycol at 37°C. The two polarization components were measured almost simultaneously in an alternating manner.

Simulations

Simulated decay data sets were generated by convoluting a nonsmoothed measured excitation profile with a sum of exponential decays. The convolution was performed by making use of the fast algorithms suggested by Grinvald et al. (11, 12). Counting error was then added according to the Gaussian asymptotic approximation of the Poisson distribution. The simulated data $y^o(t_i)$ are then given by

$$y^o(t_i) = y^c(t_i) + u\,y^c(t_i)^{1/2},$$

where the random variable u follows the standard normal distribution. The simulations were performed on a PDP 11/34 computer (Digital Equipment Corp.). The function RAN of the FORTRAN library supplied by Digital Equipment Corp., was used at the start of the noise generating sequence to give uniformly distributed random numbers on]0, 1[. The required Gaussian distributed random numbers, u, were then obtained with an algorithm according to Moshman (13). The instrumental artifacts such as scatter and time-shift, were simulated by using the procedure suggested by Grinvald (12).

Data Analysis

The real and simulated data sets were analyzed with the two described Laplace methods, LAP1 and LAP2 (see also Appendices A–D). The transformation parameters, s_j, were equidistant. The numerical integration procedure is not so important because the model parameter values are more influenced by the choice of s_j. The Simpson integration rule was used in this work. For comparison, the decay parameters were also determined by the NLLS method, using the nonlinear least-squares algorithm according to Marquardt (14) and using Gaussian weights. When NLLS was used in the analysis of the depolarization experiment, the two data sets were considered simultaneously, following the procedure suggested by C. W. Gilbert and communicated by Dale (15). The iterations in NLLS and LAP1 were terminated when the stopping rule suggested by Gallant (16) was satisfied. All the programs have been implemented in FORTRAN and use double precision arithmetic.

RESULTS AND DISCUSSION

From a critical review of Mc Kinnon et al. (1), the Laplace deconvolution could be accurate for a bi-exponential decay only if the excitation pulse has no long tail and the cut-off correction is insignificant. The suggested modification of the original Laplace deconvolution (LAP2) extends the capabilities of this method beyond these restrictions without the need of an iterative procedure. These performances will be illustrated on some real and simulated data sets with rather extreme values of the parameters. All the examples were analyzed with LAP1, LAP2, and NLLS. The latter method was used to provide statistically justified standard deviations (3) on the parameter values, providing an idea on the attainable accuracy.

As a first test for LAP2, the bi-exponential example published by Gafni et al. (5) was mimicked by simulation ($a_1 = 0.1$ ns^{-1}, $\tau_1 = 4.84$ ns, $a_2 = 0.1$ ns^{-1}, $\tau_2 = 10.32$ ns, $W = 0.196$ ns, $N = 510$, excitation profile full-width at half maximum [FWHM] = 3.5 ns). With the values of s_j suggested by Gafni (5), the parameters were very well recovered by LAP1 and LAP2. The original method, LAP1, converged within 7 to 11 iterations in contrast to LAP2, which is a single-step algorithm. In both methods, the variation of the parameters with s_j was as described by Gafni et al. (5) and was within the range limited by the support plane intervals (17) obtained by NLLS.

The same lamp profile with the same number of channels was then used in the simulation of a significant more difficult case (Simulation A). The ratio τ_1:τ_2 was halved and a_1:a_2 increased to 20 (see Fig. 1). The analyses were performed for several total numbers of channels. The results are summarized in Table I. It can be concluded that

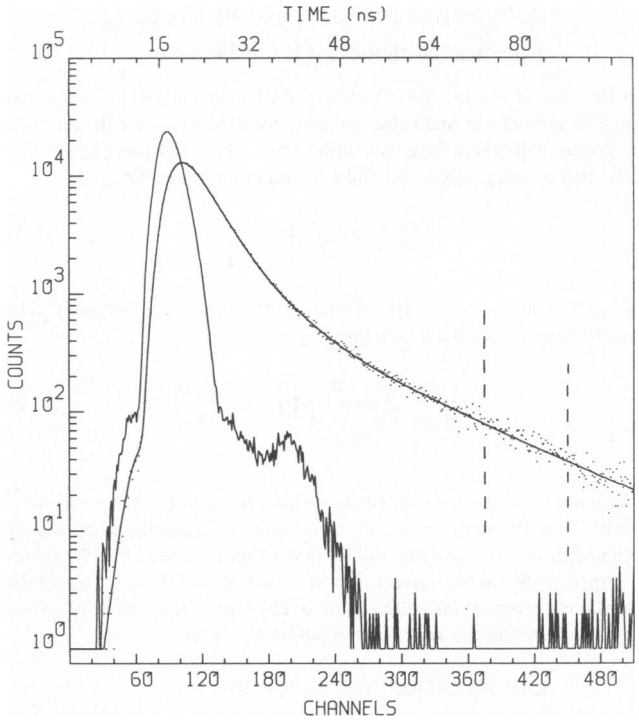

FIGURE 1 Data representation of Simulation A (Table I). The measured excitation profile (FWHM = 3.5 ns) and the fitting curve are indicated with a solid line (—). The dots (·.·) indicate the simulated decay using the parameters $a_1 = 0.2$ ns^{-1}, $\tau_1 = 4.84$ ns, $a_2 = 0.01$ ns^{-1}, and $\tau_2 = 20$ ns. The different time windows considered in Table I are indicated.

for a reduced time window the number of iterations increases significantly for LAP1. LAP2 provides, within a single step, almost the same results that remain in the confidence intervals imposed by NLLS. However, note that the high number of iterations for LAP1 is also due to the rigorous convergence criterion used. This number can be reduced by considering the data in the last channels following a procedure suggested by Gafni et al. (5).

To test the effect of the lamp profile, a simulation has been performed by using the decay parameters mentioned in the review of Mc Kinnon et al. (1) (Simulation B: $\tau_1 = 1.10$ ns, $\tau_2 = 4.89$ ns; see Fig. 2). The results of the different analyses are given in Table II. For some sets of s_j, LAP1 yielded negative parameter values after the first step. Significant values were then obtained by considering only the positive model parameters in the calculation of the cut-off correction, as already mentioned. Such problems do not arise with LAP2. As can be concluded again from Table II, LAP2 in a single step gives the same results as LAP1. Both results are comparable with the least-squares estimates.

As a final test on a bi-exponential decay, a considerable scatter artifact was included in the analysis of Simulation C (Table III). The artifact was several times greater than the contribution of the decay component with the smallest lifetime. Table III shows the results of the various analyses. As expected, the standard deviation of the smallest lifetime

TABLE I
ANALYSIS OF SIMULATION A AS REPRESENTED IN FIG. 1
(W = 0.196 ns, FWHM OF EXCITATION PROFILE = 3.5 ns)*

	N	s_1	$\Delta = s_{j+1} - s_j$	a_1	a_2	τ_1	τ_2	Stepnumber‡
		ns^{-1}	ns^{-1}	ns^{-1}	ns^{-1}	ns	ns	
Simulation	510	—	—	0.2000	0.0100	4.84	20	—
NLLS	510	—	—	0.1998	0.0102	4.82	19.8	—
	—	—	—	(0.0005)§	(0.0002)§	(0.02)§	(0.2)§	—
LAP1	—	0	0.002	0.2003	0.0104	4.80	19.8	53
	—	0	0.005	0.2003	0.0104	4.80	19.8	42
	—	0	0.01	0.2003	0.0103	4.80	19.8	31
	—	0	0.02	0.2003	0.0104	4.80	19.8	20
LAP2	—	0	0.002	0.2003	0.0103	4.81	19.9	1
	—	0	0.005	0.2003	0.0104	4.80	19.8	1
	—	0	0.01	0.2002	0.0105	4.80	19.7	1
	—	0	0.02	0.2000	0.0109	4.78	19.3	1
NLLS	451	—	—	0.1999	0.0099	4.84	20.1	—
	—	—	—	(0.0004)§	(0.0003)§	(0.02)§	(0.2)§	—
LAP1	—	0	0.002	0.2005	0.0098	4.83	20.3	107
	—	0	0.005	0.2005	0.0099	4.83	20.3	82
	—	0	0.01	0.2005	0.0099	4.82	20.2	57
	—	0	0.02	0.2004	0.0101	4.81	20.1	34
LAP2	—	0	0.002	0.2003	0.0103	4.81	19.9	1
	—	0	0.005	0.2003	0.0104	4.80	19.8	1
	—	0	0.01	0.2002	0.0106	4.80	19.6	1
	—	0	0.02	0.1998	0.0111	4.78	19.1	1
NLLS	375	—	—	0.1998	0.0103	4.82	19.7	—
	—	—	—	(0.0005)§	(0.0004)§	(0.02)§	(0.3)§	—
LAP1	—	0	0.002	0.2002	0.0105	4.80	19.7	268
	—	0	0.005	0.2001	0.0105	4.80	19.6	205
	—	0	0.01	0.2001	0.0105	4.80	19.6	140
	—	0	0.02	0.2001	0.0162	4.80	19.5	79
LAP2	—	0	0.002	0.2000	0.0107	4.80	19.4	1
	—	0	0.005	0.2000	0.0108	4.79	19.3	1
	—	0	0.01	0.1998	0.0110	4.78	19.1	1
	—	0	0.02	0.1994	0.0115	4.77	18.6	1

*The deconvolution procedures are indicated as follows: NLLS (reconvolution method based on a nonlinear least-squares search method due to Marquardt [14], LAP1 (original Laplace deconvolution method implemented with the described general solution and a modification in the calculation of the cut-off correction; see text), LAP2 (new single-step Laplace deconvolution; see text). Other notations are: N (the number of data channels considered in the convolution), W (the channel width), and the lamp full width at half maximum (FWHM) of the measured excitation profile.

‡The number of steps in the procedure required to obtain the corresponding parameter set. In Table II, the values obtained from the first step in the iterative method, LAP1, are also indicated. The number of iterations of NLLS is not indicated because it depends on the choice of starting values of the parameters.

§The standard deviations of the parameters obtained by NLLS.

is increased. LAP1 fails while LAP2 gives reasonable parameter values as compared with the NLLS results.

Although not discussed by Mc Kinnon et al. (1) and O'Connor et al. (2), it is possible to deconvolute a sum of three exponentials. With respect to this problem, the power of both Laplace deconvolutions has been investigated on some real experiments. These real data sets were first completely analyzed by NLLS and the resulting statistics indicate that only a three component model can be accepted (3). The first experiment to be discussed is the decay of 1,3-di(β-nafthoxy)-propane in iso-octane at room temperature (see also Materials and Methods). Fig. 3, showing the measured decay, clearly indicates that the Laplace transforms on these data will need a significant cut-off correction. The performances of the different analyses are shown in Table IV. Again the same conclusion can be drawn. The single-step algorithm LAP2 yields the same results in one step as does LAP1 after a relatively large number of iterations.

The performances of the deconvolution methods in the presence of the time-shift artifact were examined on a measurement of the fluorescence decay of DPAA in DPPC vesicles (see Table V and Fig. 4). The amount of the shift was determined from a measurement of a degassed solution of anthracene in cyclohexane and appeared to be ~0.12 ns. This value was then used in LAP1 and LAP2. The parameter values obtained are compared in Table V with the results of NLLS, in which the time-shift, Q, was

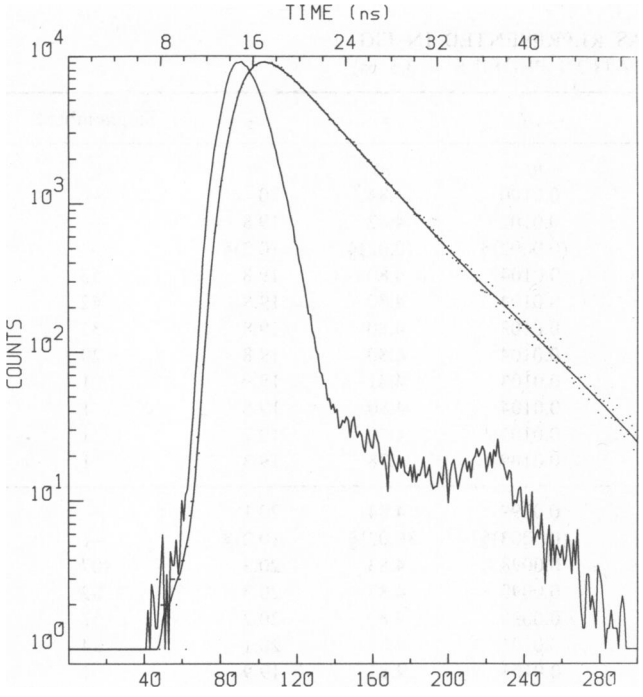

FIGURE 2 Data representation of Simulation B (Table II). The measured excitation profile and the fitting curve are indicated with a solid line (—). The dots (·.·) indicate the decay simulated with the parameters a_1 = 0.03 ns^{-1}, τ_1 = 1.10 ns, a_2 = 0.2 ns^{-1}, and τ_2 = 4.89 ns.

considered to be a free adjustable parameter. The results are in very good agreement with each other.

The performances of the new depolarization data analysis by the combination method (see Appendix D) were tested on the measurement of $r(t)$ of rhodamine 6G in propylene glycol at 37° (Table VI). Because of the large difference between the excitation and emission wavelength, 339 nm and 555 nm, respectively, the time-shift was first determined by a separate measurement of the total fluorescence emission. The obtained value of 0.3 ns was then used in the NLLS method by shifting the lamp profile and in the LAP2 analysis in the same way as described before. The results are summarized in Table VI. Both methods yield almost the same parameter values. However, it should be stressed that the Laplace method does not require the determination of the matching factor γ between the two polarization components.

To demonstrate the usefulness of the combination method on more complex anisotropies, we tried to analyze a depolarization experiment of 1,6-diphenyl-1,3,5-hexatriene (DPH) embedded in *L*-α-dimyristoylphosphatidylcholine (DMPC) vesicles above the transition temperature. Only the least-squares method yielded parameter values corresponding to the literature (10). The Laplace method failed even when applied to simulated data sets generated by using the least-squares estimates. This is due to the presence of the two fluorescence lifetimes of DPH. Proba-

TABLE II
ANALYSIS OF SIMULATION B AS REPRESENTED IN FIG. 2
(W = 0.165 ns, N = 300, LAMP FWHM = 3.5 ns)*

	s_1	$\Delta = s_{j+1} - s_j$	a_1	a_2	τ_1	τ_2	Stepnumber‡
	ns^{-1}	ns^{-1}	ns^{-1}	ns^{-1}	ns	ns	
Simulation	—	—	0.030	0.200	1.1	4.89	—
NLLS	—	—	0.033	0.199	1.1	4.89	—
	—	—	(0.003)§	(0.002)§	(0.2)§	(0.02)§	—
LAP1	0	0.01	-0.95×10^{-7}	0.214	−29.8	4.71	1
	—	—	0.035	0.198	1.0	4.90	13
	0.01	0.01	-0.16×10^{-4}	0.214	−11.6	4.72	1
	—	—	0.035	0.198	1.1	4.90	12
	0.05	0.01	-0.36×10^{-2}	0.211	−1.6	4.76	1
	—	—	0.035	0.198	1.1	4.90	8
	0.1	0.01	0.057	0.205	0.3	4.83	1
	—	—	0.035	0.198	1.0	4.90	6
	0.15	0.01	0.035	0.201	0.9	4.87	1
	—	—	0.035	0.198	1.1	4.91	5
	0.2	0.01	0.035	0.198	1.1	4.91	1
	—	—	0.035	0.197	1.1	4.92	4
LAP2	0	0.001	0.035	0.198	1.1	4.91	1
	0	0.002	0.035	0.198	1.1	4.90	1
	0	0.005	0.035	0.198	1.1	4.90	1
	0	0.01	0.035	0.198	1.0	4.90	1
	0.01	0.01	0.035	0.199	1.0	4.90	1
	0.05	0.01	0.035	0.199	1.0	4.90	1
	0.1	0.01	0.035	0.198	1.1	4.91	1
	0.15	0.01	0.036	0.197	1.2	4.93	1

*‡§See corresponding footnotes of Table I.

TABLE III
ANALYSIS OF SIMULATION C (W = 0.165 ns, N = 300, LAMP FWHM = 3.5 ns)*

	s_1	$\Delta = s_{j+1} - s_j$	a_1	a_2	τ_1	τ_2	Scatter fraction	Stepnumber‡
			ns^{-1}	ns^{-1}	ns	ns		
Simulation	—	—	0.030	0.200	1.1	4.89	0.200	—
NLLS	—	—	0.018	0.202	1.3	4.87	0.207	—
	—	—	(0.007)§	(0.002)§	(0.6)§	(0.02)§	(0.004)§	—
LAP1	0	0.01	0.001	0.204	−1.82	4.86	0.222	23
	0.01	0.01	0.035	0.204	−1.17	4.86	0.225	17
	0.05	0.01	1.828	0.204	0.07	4.86	0.088	12
	0.1	0.01	0.058	0.203	0.49	4.87	0.196	8
	0.15	0.01	0.147	0.203	0.27	4.86	0.183	6
	0.2	0.01	0.044	0.205	−0.34	4.85	0.235	5
LAP2	0.002	0.002	0.026	0.202	0.88	4.88	0.204	1
	0.005	0.005	0.029	0.202	0.82	4.88	0.203	1
	0.01	0.01	0.028	0.202	0.83	4.88	0.203	1
	0.05	0.01	0.035	0.203	0.70	4.87	0.201	1

*‡§See corresponding footnotes of Table I.

bly, most of the probes embedded in membranes will show a multiexponential behavior of the total fluorescence due to the microheterogeneity. This may restrict the use of the combination method in the analysis of the fluorescence anisotropy in membrane research. However, a depolarization experiment was simulated (Simulation G) by using the average fluorescence lifetime and the rotational correlation times of DPH in DMPC found in the literature (10). The two data sets were first analyzed separately by LAP2. In each analysis, the apparent decay constants, λ_i, were determined from the functions D_i, obtained by solving a system of three equations as described in Appendix D. Table VII clearly shows the discrepancy between the obtained parameters, λ_i, and the corresponding values calculated from τ, ϕ_1, and ϕ_2, used in the simulation. By combining the equations used in the separate analysis, we improved the result (see Appendix D). The best values result when two equations are constructed from the parallel component. Table VI shows the result for some combinations. The parameters of the simulation are well recovered with the Laplace method.

Because most anisotropy decays of DPH embedded in membranes include a limiting anisotropy, r_∞, we simulated a depolarization experiment of DPH in egg lecithin, using the parameter values obtained by Dale et al. (18) (Simulation H). Again, the average fluorescence lifetime was used. Table VIII summarizes the results for both the NLLS and the Laplace method. The parameters β_1, β_2, and r_∞ were calculated according to Eqs. D3 and D4 (Appendix D). The relatively large standard deviations, resulting from the NLLS analysis, give an indication of the difficulty of the analysis. Table VIII shows the combination method provides, within a single step, parameter values within the confidence intervals given by the NLLS method.

It can be concluded that the parameter values resulting

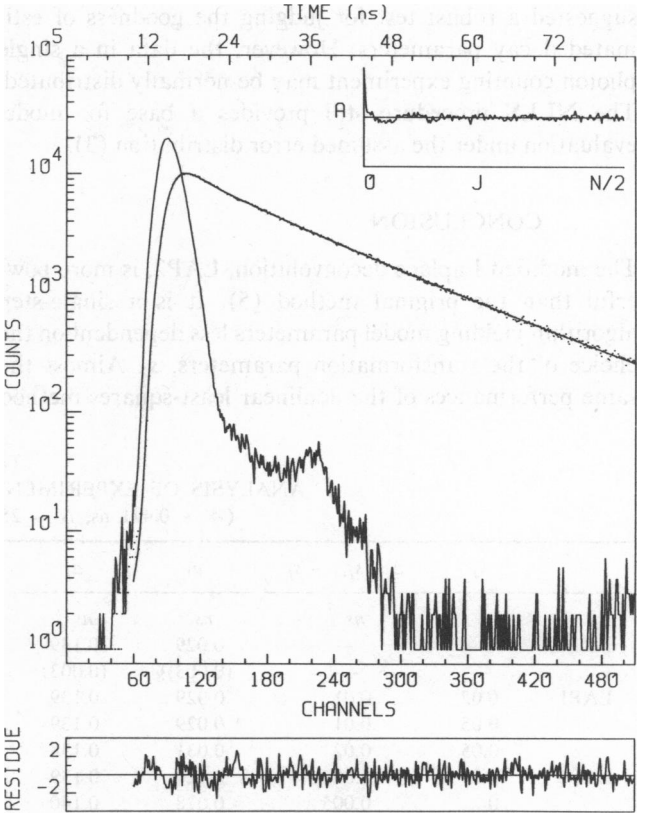

FIGURE 3 The decay of 1,3-di (β-nafthoxy)-propane in iso-octane at room temperature (data of Table III); λ_{exc} = 280 nm, λ_{em} = 335 nm. The measured excitation profile and the fitting curve are indicated with a solid line (—). The dots indicate the measured decay. The weighted residuals (RESIDUE) and their autocorrelation (A) are also shown.

TABLE IV
ANALYSIS OF EXPERIMENT D AS REPRESENTED IN FIG. 1
(W = 0.165 ns, N = 510, LAMP FWHM = 3.5 ns)*

	s_1	$\Delta = s_{j+1} - s_j$	a_1	a_2	a_3	τ_1	τ_2	τ_3	Stepnumber‡
			ns^{-1}	ns^{-1}	ns^{-1}	ns	ns	ns	
NLLS	—	—	0.062	0.06	0.08	1.8	10	20.4	—
	—	—	(0.002)§	(0.01)§	(0.01)§	(0.1)§	(1)§	(0.7)§	—
LAP1	0.05	0.008	0.063	0.05	0.10	1.6	9	19.5	91
	0.05	0.01	0.063	0.05	0.11	1.6	9	19.4	52
	0.05	0.012	0.063	0.05	0.11	1.5	9	19.4	42
	0.05	0.015	0.062	0.04	0.11	1.5	8	19.3	35
LAP2	0	0.002	0.066	0.08	0.06	2.0	13	21.9	1
	0	0.003	0.064	0.05	0.10	1.7	10	19.7	1
	0	0.004	0.064	0.05	0.10	1.7	9	19.6	1
	0	0.005	0.063	0.05	0.10	1.6	9	19.5	1

*‡§See corresponding footnotes of Table I.

from LAP2 for various values of the transformation parameter s are similar. This indicates the robustness for this method. Similar conclusions were drawn for the related transform method of moments (19, and references therein). The statistics of the parameter values obtained by the method of moments are carefully analyzed by Isenberg (20). A similar method may be followed for the Laplace transform. Very recently, Isenberg and Small (19) have suggested a robust test for judging the goodness of estimated decay parameters. However, the data in a single photon counting experiment may be normally distributed. The NLLS procedure still provides a base for model evaluation under the assumed error distribution (3).

CONCLUSION

The modified Laplace deconvolution, LAP2, is more powerful than the original method (5). It is a single-step algorithm yielding model parameters less dependent on the choice of the transformation parameters, s_j. Almost the same performances of the nonlinear least-squares method are obtained. The latter, however, provides the statistics necessary for a model building procedure (3). If the fluorescence decay is described by a single exponential, the Laplace combination method presented can be used in the analysis of a time-dependent depolarization experiment. The two polarization components can be combined in a single-step analysis without the necessity of matching. This is in contrast with earlier methods for the analysis of anisotropy decays (15, 21, 22).

APPENDIX A

Generalized Expressions for the Solution of the Nonlinear Equations Involved in the Original Laplace Deconvolution

No Artifacts Considered. The nonlinear equations solved for n relaxation constants are

$$\frac{G(s_j)}{L(s_j)} = \sum_{i=1}^{n} \frac{a_i}{s_j + \frac{1}{\tau_i}} \qquad j = 1, \ldots, 2n. \qquad \text{(A1)}$$

TABLE V
ANALYSIS OF EXPERIMENT E AS REPRESENTED IN FIG. 4
(W = 0.471 ns, N = 254, LAMP FWHM = 3.5 ns)*

	s_1	$\Delta = s_{j+1} - s_j$	a_1	a_2	a_3	τ_1	τ_2	τ_3	Q‖	Stepnumber‡
	ns^{-1}	ns^{-1}	ns^{-1}	ns^{-1}	ns^{-1}	ns	ns	ns	ns	
NLLS	—	—	0.029	0.139	0.0016	2.6	8.8	37	0.13	—
	—	—	(0.003)§	(0.003)	(0.0003)	(0.5)	(0.1)	(4)	(0.02)	—
LAP1	0.02	0.01	0.029	0.139	0.0016	2.6	8.8	38	0.12	93
	0.05	0.01	0.029	0.139	0.0016	2.5	8.8	38	0.12	21
	0.05	0.02	0.031	0.138	0.0011	2.7	8.9	46	0.12	15
LAP2	0	0.002	0.029	0.139	0.0016	2.6	8.8	39	0.12	1
	0	0.005	0.028	0.140	0.0016	2.5	8.8	38	0.12	1
	0	0.01	0.028	0.140	0.0016	2.5	8.8	38	0.12	1
	0	0.013	0.029	0.139	0.0014	2.6	8.9	40	0.12	1

*‡§See corresponding footnotes of Table I.

‖The time-shift Q was a free adjustable parameter in NLLS, while the value of 0.12 ns for the Laplace deconvolutions was determined from the anthracene standard.

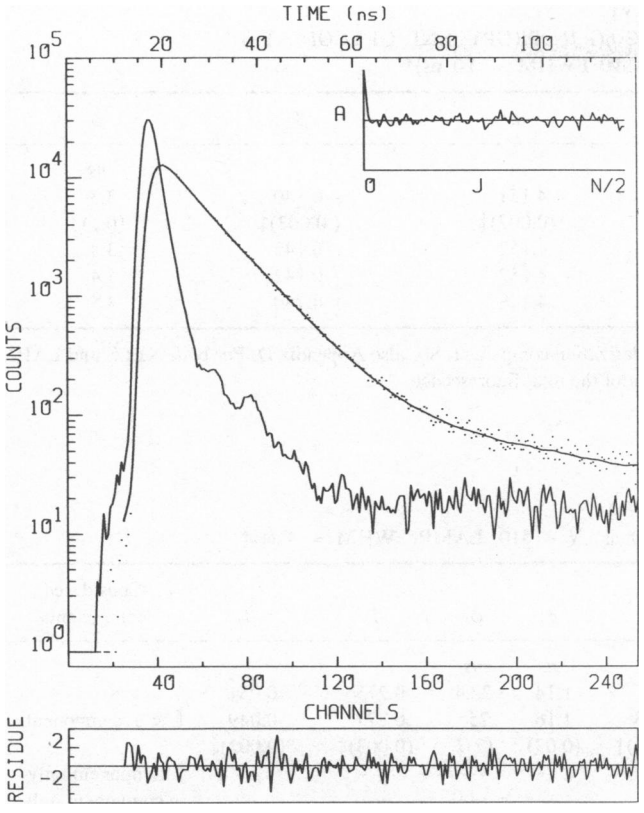

FIGURE 4 The decay of DPAA is DPPC vesicles at 33°C (data of Table V); λ_{exc} = 358 nm, λ_{em} = 425 nm. The excitation light was vertically polarized and the analyzer at the emission side was oriented at 55° with respect to the vertical. The measured excitation profile and the fitting curve are indicated with a solid line (—). The dots (˙.˙) indicate the measured decay. The weighted residuals (RESIDUE) and their autocorrelation (A) are also shown.

Eq. A1 can be written in the form

$$L(s_j)\sum_{i=1}^{n} s_j^{i-1} E_i(a,\tau) - G(s_j)\sum_{i=1}^{n} s_j^i D_i(\tau) = G(s_j)$$

with

$$D_1(\tau) = \sum_i \tau_i$$

$$D_2(\tau) = \sum_{i>j} \tau_i\tau_j$$

$$D_3(\tau) = \sum_{i>j>k} \tau_i\tau_j\tau_k$$

etc . . .

and

$$E_1(a,\tau) = \sum_i a_i\tau_i$$

$$E_2(a,\tau) = \sum_{i>j} (a_i + a_j)\,\tau_i\tau_j$$

$$E_3(a,\tau) = \sum_{i>j>k} (a_i + a_j + a_k)\,\tau_i\tau_j\tau_k.$$

etc . . .

The functions D_i and E_i can now be determined from a system of linear equations. The lifetimes, τ_i, are the roots of the polynomial of degree n,

$$\sum_{i=0}^{n} (-1)^i D_i \tau^{n-i} \qquad (D_0 \equiv 1).$$

Once $\{\tau_j\}$ determined, $\{a_j\}$ can be readily obtained from $\{E_i\}$.

Observed Decay Contains a Scatter Component S_c.

The system of equations solved takes the form

$$\frac{G(s_j)}{L(s_j)} = \sum_{i=1}^{n} \frac{a_i}{s_j + \frac{1}{\tau_i}} + S_c \quad j = 1, \ldots, (2n+1). \qquad \text{(A2)}$$

The equation can be rewritten as

$$L(s_j)\,s_j^n D_n(\tau) S_c + L(s_j)\sum_{i=1}^{n} s_j^{i-1} K_i(a,\tau,S_c) - G(s_j)\sum_{i=1}^{n} s_j^i D_i(\tau) = G(s_j),$$

with

$$K_i(a,\tau,S_c) = E_i(a,\tau) + S_c D_{i-1}(\tau) \qquad (D_0 \equiv 1)$$

Determination of $D_n(\tau)S_c$, $K_i(a,\tau,S_c)$ and $D_i(\tau)$ leads to the final solution for S_c, a_i, and τ_i.

The Lamp and the Decay Curve Shifted with Respect to Each Other by an Amount Q.

$$\frac{G(s_j)}{L(s_j)} = e^{-Qs_j}\sum_{i=1}^{n} \frac{a_i}{s_j + \frac{1}{\tau_i}}.$$

When the time-shift Q is determined from a separate experiment, one can define

$$G_Q(s_j) = G(s_j)\,e^{Qs_j}.$$

The unknown a_j and τ_j can now be determined by replacing $G(s_j)$ by $G_Q(s_j)$ in the section *No Artifacts Considered.*

APPENDIX B

Expressions Involved in the Alternative Laplace Deconvolution

No Artifacts Considered. The unknown a_i, τ_i, and c_i have to be determined from

$$\frac{G^T(s_j)}{L^T(s_j)} = \sum_{i=1}^{n} \frac{a_i}{s_j + \frac{1}{\tau_i}}\left[1 - \frac{e^{-s_jT}c_i}{L^T(s_j)}\right] \qquad j = 1, \ldots, 3n. \qquad \text{(B1)}$$

Rewriting leads to

$$L^T(s_j)\sum_{i=1}^{n} s_j^{i-1} E_i(a,\tau) - e^{-s_jT}\sum_{i=1}^{n} s_j^{i-1} H_i(a,\tau,c) - G^T(s_j)\sum_{i=1}^{n} s_j^i D_i(\tau) = G^T(s_j),$$

TABLE VI

ANALYSIS OF EXPERIMENT F: RHODAMINE 6G IN PROPYLENE GLYCOL AT 37°C

(W = 0.160 ns, N = 254, LAMP FWHM = 3.0 ns)*

	s_1	$\Delta = s_{j+1} - s_j$	τ	β	ϕ
	ns^{-1}	ns^{-1}	ns		ns
NLLS	—	—	4.151	−0.140	3.3
	—	—	(0.007)‡	(0.003)‡	(0.1)‡
LAP2	0	0.002	4.152	−0.143	3.4
Combination	0.002	0.002	4.152	−0.142	3.4
	0.01	0.01	4.148	−0.140	3.5

In the LAP2 combination method, one equation is constructed from each polarization component. See also Appendix D. For both NLLS and LAP2, the time-shift Q was taken equal to 0.3 ns, as determined from the measurement of the total fluorescence.

*See corresponding footnote in Table I.

‡The standard deviations of the parameters obtained by NLLS.

TABLE VII

ANALYSIS OF SIMULATION G (W = 0.070 ns, N = 510, LAMP FWHM = 3 ns)*

	s_1	$\Delta = s_{j+1} - s_j$	λ_1	λ_2	λ_3	τ	ϕ_1	ϕ_2	β_1	β_2	Considered components
	ns^{-1}	ns^{-1}	ns	ns	ns	ns	ns	ns			
Simulation	—	—	7.6	0.991	5.67	7.6	1.14	22.4	0.275	0.051	
NLLS	—	—	—	—	—	7.603	1.16	25	0.277	0.049	∥ & ⊥ component
	—	—	—	—	—	(0.005)‡	(0.03)	(2)‡	(0.003)‡	(0.002)‡	
LAP2	0.002	0.008	8.618	0.997	7.167	—	—	—	—	—	∥ component only
Combination	—	—	7.674	−0.554	1.040	—	—	—	—	—	⊥ component only
	—	—	7.608	0.989	5.501	7.608	1.14	20	0.273	0.053	∥1, ∥3, ⊥1
	—	—	7.608	0.989	5.492	7.608	1.14	20	0.273	0.052	∥1, ∥2, ⊥1
	—	—	7.606	0.989	5,484	7.606	1.14	20	0.273	0.052	∥2, ∥3, ⊥3
	—	—	7.606	0.989	5.465	7.606	1.14	20	0.272	0.051	∥1, ∥2, ⊥3
	—	—	7.611	1.009	6.085	7.611	1.16	30	0.283	0.065	∥1, ⊥2, ⊥1
LAP2	0.0001	0.01	9.781	0.999	7.304	—	—	—	—	—	∥ component only
Combination	—	—	7.673	−0.246	1.046	—	—	—	—	—	⊥ component only
	—	—	7.608	0.989	5.498	7.608	1.14	20	0.273	0.053	∥1, ∥2, ⊥1
	—	—	7.606	0.990	5.496	7.606	1.14	20	0.273	0.051	∥1, ∥3, ⊥2
	—	—	7.605	0.990	5.493	7.605	1.14	20	0.272	0.051	∥2, ∥3, ⊥3
	—	—	7.608	0.990	5.528	7.608	1.14	20	0.273	0.053	∥2, ∥3, ⊥1
	—	—	7.610	1.010	6.147	7.610	1.16	32	0.284	0.067	∥1, ⊥1, ⊥2

The data sets from which the equations are constructed for the LAP2 combination method are indicated in the last column. The pre-exponentials β_j were obtained from the parallel component. See also Appendix D. The apparent decay constants, λ_i, in the table for the simulation are calculated from τ, ϕ_1, and ϕ_2.

*See corresponding footnote of Table I.

‡The standard deviation of the parameters obtained by NLLS.

TABLE VIII

ANALYSIS OF SIMULATION H (W = 0.070 ns, N = 510, LAMP FWHM = 3 ns)*

	s_1	$\Delta = s_{j+1} - s_j$	τ	β_1	β_2	r_∞	Φ_1	Φ_2
	ns^{-1}	ns^{-1}	ns	ns	ns		ns	ns
Simulation	—	—	8.060	0.162	0.144	0.044	2.1	8.8
NLLS	—	—	8.064	0.17	0.13	0.044	2.2	9
	—	—	(0.004)‡	(0.02)‡	(0.02)‡	(0.004)‡	(0.2)‡	(2)‡
LAP2	0.002	0.008	8.054	0.18	0.13	0.045	2.3	10
Combination	0.01	0.01	8.054	0.17	0.14	0.047	2.3	10
	0.05	0.01	8.046	0.16	0.14	0.053	2.1	8

*In the LAP2 combination method, two equations were constructed from the parallel component and the third from the perpendicular polarization. See also Appendix D.

‡The standard deviation of the parameters obtained by NLLS.

with

$$H_1(a, \tau, c) = \sum_i a_i c_i \tau_i$$

$$H_2(a, \tau, c) = \sum_{i>j} (a_i c_i + a_j c_j)\tau_i \tau_j$$

$$H_3(a, \tau, c) = \sum_{i>j>k} (a_i c_i + a_j c_j + a_k c_k)\tau_i \tau_j \tau_k$$

etc . . . .

D_i and E_i are as defined in the Appendix A section *No Artifacts Considered*. From these equations the functions D_i, E_i, and H_i may be obtained directly. However, the coefficients of the matrix used in that procedure may differ largely and inaccurate values for a_j, τ_j, and c_j may result. The following step should be preferred to eliminate the parameters c_i. We define a linear operator M_i on the Laplace transforms,

$$M_i[K(s_j)] = K(s_j)s_j^i + n\sum_{k-1}^{n-1} (-1)^k e^{\Delta T} K(s_{j+k})\, s_{j+k}^i + (-1)^n e^{n\Delta T} K(s_{j+n})\, s_{j+n}^i,$$

where $K(s_j)$ stands for $G^T(s_j)$ or $L^T(s_j)$ and $s_{j+1} = s_j + \Delta$. The final equations solved have the form

$$\sum_{i-1}^{n-1} M_{i-1}\,[L^T(s_j)]E_i(a,\tau) - \sum_{i-1}^{n} M_i[G^T(s_j)]D_i(\tau) = M_0[G^T(s_j)] \qquad j = 1, \ldots, 2n. \quad \text{(B2)}$$

The parameters a_j and τ_j are determined from D_i and E_i as described before.

Correction for a Scatter Component S_c. The scatter correction should result from

$$\frac{G^T(s_j)}{L^T(s_j)} = \sum_{i-1}^{n} \frac{a_i}{s_j + \dfrac{1}{\tau_i}}\left[1 - \frac{e^{-s_j T} c_i}{L^T(s_j)}\right] + S_c. \quad \text{(B3)}$$

By using the linearity of the operator M_i, one obtains

$$M_n[L^T(s_j)]\, S_c D_n + \sum_{i-1}^{n-1} M_i[L^T(s_j)]\, K_i(a, \tau, S_c) - \sum_{i-1}^{n} M_i\,[G^T(s_j)]D_i(\tau) = M_0[G^T(s_j)],$$

with the functions $K_i\,(a, \tau, S_c)$ defined as before.

Correction for Time-Shift Error Q. Obviously, the system of equation to be solved is given by

$$\frac{G^T(s_j)}{L^T(s_j)} = e^{-Qs_j} \sum_{i-1}^{n} \frac{a_i}{s_j + \dfrac{1}{\tau_i}}\left[1 - \frac{e^{-s_j T} c_i}{L^T(s_j)}\right]. \quad \text{(B4)}$$

When the time-shift Q is known, one can define

$$G_Q^T(s_j) = e^{Qs_j} G^T(s_j)$$

and construct $M_i\,[G_Q^T(s_j)]$. The parameters can then be determined as from Eq. B2.

APPENDIX C

Expressions for the Combination of Several Experiments by Using the Alternative Laplace Deconvolution

To eliminate the need for normalization factors between the experiments, the functions $E_i(a, \tau)$ have to be eliminated first from Eq. B2. This is done by substituting the formal solution for the functions, $E_i(a, \tau)$, from the first n equations into the $(n + 1)^{\text{th}}$ equation. The latter can then be written as

$$\begin{vmatrix} \sum_{i-0}^{n} M_i\,[G^T(s_j)]\, D_i & M_{n-1}\,[L^T(s_j)] & \cdots & M_0\,[L^T(s_j)] \\ \vdots & \vdots & & \vdots \\ \sum_{i-0}^{n} M_i\,[G^T(s_{j+n})]\, D_i & M_{n-1}\,[L^T(s_{j+n})] & \cdots & M_0\,[L^T(s_{j+n})] \end{vmatrix} = 0, \quad \text{(C1)}$$

(C1)

with $D_0 \equiv 1$. By developing this expression, one obtains

$$\sum_{i-1}^{n} \begin{vmatrix} M_i\,[G^T(s_j)] & M_{n-1}\,[L^T(s_j)] & \cdots & M_0\,[L^T(s_j)] \\ \vdots & \vdots & & \vdots \\ M_i\,[G^T(s_{j+n})] & M_{n-1}\,[L^T(s_{j+n})] & \cdots & M_0\,[L^T(s_{j+n})] \end{vmatrix} D_i = -\begin{vmatrix} M_0\,[G^T(s_j)] & M_{n-1}\,[L^T(s_j)] & \cdots & M_0\,[L^T(s_j)] \\ \vdots & \vdots & & \vdots \\ M_0\,[G^T(s_{j+n})] & M_{n-1}\,[L^T(s_{j+n})] & \cdots & M_0\,[L^T(s_{j+n})] \end{vmatrix}. \quad \text{(C2)}$$

By repeating this procedure on the experiments to be combined, we obtain n linearly independent expressions like Eq. C2. From the resulting system of equations the $D_i(\tau)$ and hence τ_j can be determined. If the number of experiments is less than n, the construction has to be performed several times on a same data set. In this way, a particular experiment may be given more weight in the combination. Once the decay constants are determined, the pre-exponentials are to be calculated from one data set because no normalization was performed. A rearrangement of Eq. B1 leads to the expressions from which the a_i can be calculated

$$\sum_i a_i \left(\frac{L^T(s_j) - c_i\, e^{-T/s_j}}{s_j + \dfrac{1}{\tau_i}}\right) = G^T(s_j), \quad \text{(C3)}$$

where the corrections c_i are estimated according to

$$c_i = e^{-T/\tau_i} L^T\left(-\frac{1}{\tau_i}\right).$$

Once the pre-exponentials a_i are calculated for experiment k, the weighting factors $\alpha_{ki} = [a_i/\Sigma\, a_i]_k$ may be averaged over the experiments to elicit more accurate results.

APPENDIX D

Laplace Combination Method Applied to Time-Dependent Depolarization Experiments

The two polarization components from which the fluorescence $f(t)$ and the anisotropy $r(t)$ have to be determined can be written as

$$i_{/\!/}(t) = \frac{f(t)}{3}[1 + 2r(t)]$$

$$i_{\perp}(t) = \gamma\frac{f(t)}{3}[1 - r(t)]. \qquad \text{(D1)}$$

The experimental matching factor is denoted by γ. If the total fluorescence is exponential and the anisotropy is given by

$$r(t) = \sum_{j}^{m} \beta_j e^{-t/\phi_j} + r_\infty,$$

the Eq. D1 can be rewritten as

$$i_{/\!/}(t) = \sum_{i-1}^{m+1} e_i e^{-t/\lambda_i}$$

$$i_{\perp}(t) = \sum_{i-1}^{m+1} d_i e^{-t/\lambda_i} \qquad \text{(D2)}$$

with

$$\lambda_1 = \tau$$

$$\lambda_{i+1} = \left(\frac{1}{\tau} + \frac{1}{\phi_i}\right)^{-1}$$

$$e_1 = \frac{a}{3}(1 + 2r_\infty) \qquad d_1 = \gamma\frac{a}{3}(1 - r_\infty)$$

$$e_{i+1} = \frac{2}{3}a\beta_i \qquad d_{i+1} = -\gamma\frac{a}{3}\beta_i.$$

The two data sets, $i_{/\!/}(t)$ and $i_{\perp}(t)$, have the same apparent decay constants λ_i, so that the combination method of Appendix C can be applied. Note that the fluorescence lifetime corresponds to the largest λ_i. If a limiting anisotropy r_∞ is not considered, the factors β_i can be determined from a single data set. We found that the data of $i_{/\!/}(t)$ is preferred. In the other situation, we suggest the following formulas in which the factor γ disappears

$$\beta_i = \frac{3}{2\left(\frac{e_1}{e_{i+1}} - \frac{d_1}{d_{i+1}}\right)} \qquad \text{(D3)}$$

$$r_\infty = \frac{\frac{e_{i+1}}{2e_1} + \frac{d_{i+1}}{d_1}}{\frac{d_{i+1}}{d_1} - \frac{e_{i+1}}{e_1}}. \qquad \text{(D4)}$$

The authors wish to thank Dr. R. Todesco, Professor J. Put, Dr. K. De Meyer, and Professor F. De Schrijver for supplying the fluorescent probes used in this work.

Received for publication 1 July 1982 and in final form 15 April 1983.

REFERENCES

1. McKinnon, A. E., A. G. Szabo, and D. R. Miller. 1977. The deconvolution of photoluminescence data. *J. Phys. Chem.* 81:1564–1570.
2. O'Connor, D. V., W. R. Ware, and J. C. Andre. 1979. Deconvolution of fluorescence decay curves. A critical comparison of techniques. *J. Phys. Chem.* 83:1333–1343.
3. Ameloot, M., and H. Hendrickx. 1982. Criteria for model evaluation in the case of deconvolution calculations. *J. Chem. Phys.* 76:4419–4432.
4. Helman, W. P. 1971. Analysis of very fast transient luminescence behavior. *Int. J. Radiat. Phys. Chem.* 3:283–294.
5. Gafni, A., R. L. Modlin, and L. Brand. 1975. Analysis of fluorescence decay curves by means of the Laplace transformation. *Biophys. J.* 15:263–280.
6. Ehrenberg, M., and R. Rigler. 1972. Polarized fluorescence and rotational Brownian motion. *Chem. Phys. Lett.* 14:539–544.
7. Kinosita, K., Jr., S. Kawato, and A. Ikegami. 1977. A theory of fluorescence polarization decay in membranes. *Biophys. J.* 20:289–305.
8. Hazan, G. H., A. Grinvald, M. Maytal, and I. Z. Steinberg. 1974. An improvement of nanosecond fluorimeters to overcome drift problems. *Rev. Sci. Instrum.* 45:1602–1604.
9. Todesco, R. 1981. Ph.D. dissertation. Photophysics and Photochemistry of Dinaphthyl Compounds. Leuven, Belgium.
10. Chen, L. A., R. E. Dale, S. Roth, and L. Brand. 1977. Nanosecond time-dependent fluorescence depolarization of diphenylhexatriene in dimyristoyllecithin vesicles and the determination of "microviscosity." *J. Biol. Chem.* 252:2163–2169.
11. Grinvald, A., and I. Z. Steinberg. 1974. On the analysis of fluorescence decay kinetics by the method of least squares. *Anal. Biochem.* 59:583–598.
12. Grinvald, A. 1976. The use of standards in the analysis of fluorescence decay data. *Anal. Biochem.* 75:260–280.
13. Moshman, J. 1967. Random number generation. *In* Mathematical Methods for Digital Computers. A. Ralston and H. S. Wilf, editors. John Wiley & Sons, Inc., New York. 249–263.
14. Marquardt, D. W. 1963. An algorithm for least-squares estimation of nonlinear parameters. *J. Soc. Ind. Appl. Math.* 11:431–441.
15. Dale, R. E. 1980. Time resolved fluorescence spectroscopy in biochemistry and biology. *In* NATO Advanced Study Institute. Plenum Publishing Corporation, London.
16. Gallant, A. R. 1975. Nonlinear Regression. *Amer. Statist.* 29:73–81.
17. Stone, H. 1960. Discussion on paper by E. M. L. Beale. *J. Roy. Statist. Soc., Ser. B.* 22:84–85.
18. Dale, R. E., L. A. Chen, and L. Brand. 1977. Rotational relaxation of the "microviscosity" probe diphenylhexatriene in paraffin oil and egg lecithin vesicles. *J. Biol. Chem.* 252:7500–7510.
19. Isenberg, I., and E. W. Small. 1982. Exponential depression as a test of estimated decay parameters. *J. Chem. Phys.* 77:2799–2805.
20. Isenberg, I. 1973. On the theory of fluorescence decay experiments. II. Statistics. *J. Chem. Phys.* 59:5708–5713.
21. Wahl, Ph. 1977. Statistical accuracy of rotational correlation times determined by the photoncounting pulse fluorimetry. *Chem. Phys. Lett.* 22:245–256.
22. Wahl, Ph. 1979. Analysis of fluorescence anisotropy decays by a least square method. *Biophys. Chem.* 10:91–104.